Crude oil exposure reduces ice algal growth in a sea-ice mesocosm experiment

[1]Kyle Dilliplaine*, [2]Marc Oggier, [1,3]R. Eric Collins, [2]Hajo Eicken, [4]Rolf Gradinger, [1,4]Bodil A. Bluhm

[1]College of Fisheries and Ocean Sciences, University of Alaska Fairbanks, Fairbanks, Alaska, USA
[2]International Arctic Research Center, University of Alaska Fairbanks, Fairbanks, Alaska, USA
[3]Centre for Earth Observation Science, University of Manitoba, Winnipeg, Manitoba, Canada
[4]Department of Arctic and Marine Biology, UiT The Arctic University of Norway, Tromsø, Norway

*Communicating Author: kbdilliplaine@alaska.edu

Kyle Dilliplaine ORCID 0000-0001-6079-7283
Marc Oggier ORCID 0000-0003-4679-1103
R. Eric Collins ORCID 0000-0002-5858-2395
Hajo Eicken ORCID 0000-0002-9718-9406
Rolf Gradinger ORCID 0000-0001-6035-3957
Bodil A. Bluhm ORCID 0000-0002-4584-7796

Abstract: Oil production in Arctic ice-covered areas poses a risk for pollution of the ecosystem including that within the brine channel network of sea ice. Sea-ice autotrophs contribute substantially to Arctic primary production, but are inherently difficult to test for oil exposure responses *in situ*. This study had two objectives, first, we developed a suitable lab-based mesocosm system, second, we tested oil effects on sea-ice algae. Specifically, we investigated if Alaska North Slope crude oil exposure reduces ice algal abundance, biomass and concentration of extracellular polymeric substances (EPS) using indoor ice tanks over a 10-day exposure period. Six tanks in one cold room were used in pairs for the following treatments: (1) control, (2) oil release as a layer under ice and (3) release of dispersed oil. All tanks were inoculated with sea-ice microbial communities collected from Utqiaġvik, Alaska. After 10 days of exposure, the abundance of algae, dominated by the pennate diatom genus *Nitzschia*, and the concentrations of EPS and chlorophyll *a* were significantly lower in the oiled treatments compared to the control. We suggest light attenuation by the oil, reduced algal mobility, and oil toxicity as causes for this reduction. Observed changes in cell fluorescence characteristics based on DNA staining could be linked to the oil exposure and could provide a new tool for assessment of toxicity in microalgae.

Keywords: Arctic sea ice, Crude oil, Mesocosm, Ice algae, Epifluorescence microscopy
Declarations

Funding: This project was funded by a research grant provided through the Coastal Marine Institute (CMI M14AC00015), a joint institute between the Bureau of Ocean Energy Management (BOEM) and the University of Alaska Fairbanks. Additional financial support was provided by the Robert and Kathleen Byrd Award (UAF).

Conflicts of Interest: The authors declare that they have no known conflicts of interest.

Ethics approval: Not applicable

Consent to participate: Not applicable

Consent for publication: Not applicable

Availability of data and material: Private link to figshare data for use during review: https://figshare.com/s/4512e5ce721d65c3f7ad. Public doi for data will be: 10.6084/m9.figshare.11918349.

Code availability: Code for processing figures and manipulating data can be found from GitHub: https://github.com/kbdilliplaine/Crude-Oil-Experiment.git.

Introduction

The dramatic loss of Arctic sea ice (Polyakov et al. 2017) is spurring the development of Arctic marine resources including shipping lanes, fisheries, and petroleum reserves (Arctic Council 2009; Eguíluz et al. 2016). While offshore oil production in the US Arctic is constrained around Prudhoe Bay, located in Alaska's landfast ice belt (Mahoney et al. 2014), new lease sales scheduled for 2019-2023 (BOEM 2019) are also located in areas of seasonal sea-ice cover. Increased human activity, and potential oil production developments, increase the risk for oil pollution in Arctic ice-covered waters. The fate and impact of released oil on the Arctic marine environment will vary depending on, e.g., the season, weather and ice conditions at the time the event occurs (summarized in Lee et al. (2011)). Despite the expectation of ice-free summers by 2050 (Overland and Wang 2013; Wang et al. 2018), sea ice will continue to form during the Arctic winter and represent a hazard to the petroleum and maritime shipping industries, complicating the cleanup of oil spills in ice-covered waters. The fate of released oil in the marine environment is largely controlled through processes like evaporation, dispersion, sedimentation, oxidation and bioremineralization, best understood in lower latitudes. A long term *in situ* study (2.5 months) in first-year ice covered waters revealed a 1% per day removal rate for polycyclic aromatic compounds, mainly due to photooxidation and not biological processes, while removal of alkanes was much lower (Vergeynst et al. 2019). Turbulent weather conditions or high current velocities may naturally disperse oil in the upper water column (Tkalich and Chan 2002). The breakup of oil into small droplets increases the amount of hydrocarbons measured in the water, which enhances toxicity to organisms (Gardiner et al. 2013; Özhan et al. 2014). While in principle the same processes are relevant during periods of ice cover, they are modified by the presence of the fast ice or pack ice cover and the co-occurring low water temperatures. Presence of ice has a multitude of effects including, for example, the reduction of turbulent mixing in the water column and the evaporation of oil into air. The ice and snow cover provide porous media, where oil can migrate up brine channels, be encapsulated within the ice or form layers in oil pools directly at the ice water interface.

Oil spills in the Arctic will affect the entire food web. Model studies suggest, for example, that oil spills can expose large fractions of populations of polar bears to released oil in the Chukchi Sea (Wilson et al. 2018) and causes different risks to other animals, like ringed seals and walrus, based on an oil spill risk assessment for the Kara Sea (Helle et al. 2020). Arctic sea birds are also sensitive to oil pollution as demonstrated in the high mortality of guillemots and little auks off Newfoundland caused by ship-source oil pollution (Frederiksen et al. 2019). Information regarding the impacts of oil to zooplankton and phytoplankton is necessary for ecosystem level assessment (Olsen et al. 2013). Exposure of Arctic phytoplankton and zooplankton to sub-lethal concentrations of the water accommodated fraction (WAF) of oil drastically reduced their physiological rates, specifically algal primary production and zooplankton fecal pellet production (Lemcke et al. 2019). Experimental data also suggest that oil exposure can cause delayed effects on reproduction, grazing and lipid accumulation of important Arctic zooplankton taxa like *Calanus hyperboreus* (Toxværd et al. 2019) and growth and reproduction for the important Arctic fish species *Boreogadus saida* (Bender et al. 2018).

The generally weak knowledge base on the impacts of oil pollution onto Arctic marine lower trophic levels also applies to the ecosystem within sea ice. Brine channels and pockets within the ice provide habitat for a very diverse sea-ice community, consisting mainly of viruses, bacteria, archaea, microalgae, fungi, and small unicellular and multicellular heterotrophs (Bluhm et al. 2018) creating a complex ice-based food web (Gradinger and Bluhm 2020). Highest biomass and activity resides in the bottom few centimeters of Arctic sea ice largely due to the needed nutrient supply from the water column (Manes and Gradinger 2009). Algal abundance and biomass concentrations in sea ice can be up to 10-1,000 time greater than in the underlying water column at certain times of the year (Lee et al. 2008; Manes and Gradinger 2009) and provide a significant food source for pelagic and benthic fauna (Michel et al. 2006; Boetius et al. 2013). The significance of ice algae as a food source is particularly high in early spring, when ice-algal blooms contribute to zooplankton nutrition before the onset of the subsequent phytoplankton bloom (Søreide et al. 2010; Leu et al. 2015). Sea-ice algae are also a major producer of extracellular polymeric substances (EPS) (Krembs et al. 2011; Aslam et al. 2016). EPS, produced by algae and bacteria, is found in sea ice at high concentrations (Krembs et al. 2002; Underwood et al. 2013) and protects cells from freezing (Liu et al. 2013) and osmotic effects of hyper- and hyposaline environments (Ozturk and Aslim 2010; Aslam et al. 2012; Liu et al. 2013). Biologically produced EPS can directly modify the brine channel structure (Krembs et al. 2011),

effecting the flow of fluids like brine and oil through sea ice, potentially altering the exposure of ice-based organisms to oil.

Studying the effects of oil pollution on sea-ice biota is challenging given the microscale nature of the brine channel network, which is essential to be included as it determines the fate of oil in sea ice to a large extent. Oil spilled under sea ice from a well blowout or damaged vessel will rise through the water column and pool at the underside of the ice, accumulating in recesses and undulations (Glaeser and Vance 1971; Dickens et al. 1975). Oil encapsulation in growing ice can occur over one to two days (Dickens et al. 1975; Buist and Dickins 1987; Karlsson 2009), where it may either migrate through the ice at low temperatures (T_{ice}< -5 °C) (Oggier et al. 2019) or remain encapsulated until increased porosity and permeability related to spring warming allows the oil surface (Dickens et al. 1975). The high concentrations of sea-ice biota near the ice/water interface, which contribute substantially to Arctic Ocean primary production (Wiedmann et al. 2020), are particularly at risk from under-ice oil exposure. Biological effects of oil have been demonstrated in only a few earlier studies including inhibition of ice-algal growth (Delille and Fiala 1999) and/or decrease of ice meiofauna abundance (Cross and Martin 1987), but microalgal responses to oil exposure vary markedly. Direct comparisons between experimental studies are complicated by the large variability in study design, organism focus, crude-oil source and chemical composition, and exposure rates and durations. This applies also to attempts of field-based microcosm experiments (Camus and Smit 2019), where natural sea ice communities are exposed to pollutants, as species composition and biomass in natural sea ice can vary even on small scales of a few meters (Rysgaard et al. 2001) making replication in *in situ* studies intrinsically difficult.

Our study, first, addressed the methodological challenge to develop a mesocosm test system overcoming the uncertainties of field studies, while providing a standardized environment to conduct oil exposure experiments on Arctic sea-ice communities. Second, we tested two different credible oil exposure scenarios: 1) an oil release under calm conditions leading to the formation of oil lenses and 2) a release of physically dispersed oil, mimicking more turbulent conditions. This study focusses on the response of sea-ice algae to such exposure using the change over time of cell abundances, chlorophyll *a* (Chl *a*) and EPS concentrations as primary measures; physical effects in this experimental apparatus have been described in Oggier et al. (2019). We hypothesized that: A) oil exposure would reduce ice algal growth and potentially cause algal mortality, and B) dispersed oil would have a larger effect size than an oil lens due to the increased concentrations of toxins expected in the water-accommodated fraction as a result of the physical mixing process.

Methods

Tank setup

A detailed description of the basic tank setup can be found in Oggier et al. (2019). Briefly, six high density polyethylene (HDPE) tanks (Greer Tank & Welding, 1 m high and 0.36 m^2 in surface area) were fitted with a black HDPE 152 µm thick liner to avoid contamination of the tanks during oil exposure (Fig. 1). Each tank was filled with 360 L of freshwater mixed with aquarium salt blend, Instant Ocean, to an initial salinity of 26. Tanks were located in a cold room facility set to -15 °C, in which sea ice was grown to approximately 10 cm thickness before biota was added. To sustain ice algal primary production, LED lights (Reef Breeders Super Lux) covering the full photosynthetically active radiation (PAR) spectrum (400-700 nm) were hung 50 cm above the ice surface. An under-ice irradiance of 15 µmol photons m^{-2} s^{-1} was targeted in order to simulate irradiance values observed *in situ* from Arctic seasonal landfast ice zones (Gradinger et al. 2009). A spherical PAR sensor was installed in one tank and used for initial light adjustment in all tanks, however this sensor failed just before oil was released. Based on the available under-ice light data and results from trial runs (data not shown), the surface PAR (measured with planar PAR sensor) was increased daily by 3 µmol photons m^{-2} s^{-1} to counteract increasing attenuation from the growing ice sheet to keep a near constant under-ice PAR. A thin optically-neutral film (12.5 µm thickness) of transparent plastic (PVC, Reynolds) was placed over the ice surface of each tank to reduce water sublimation and thus burden on the freezer compressor. The temperatures of air, ice surface (Fisher Scientific, Traceable Thermometer), and water salinity (YSI EcoSense EC300A), were recorded every 1-3 days (Online Resources 1 and 2) concurrent with irradiance measurements.

146

147 *Inoculation of ice biota into the mesocosms*

148 In March of 2015, ice biota was collected from level landfast sea ice close to Utqiaġvik, Alaska for use as an
149 inoculum within the tanks. The bottom 1-3 cm of ice from sixty-four ice cores of 20-cm diameter, containing the
150 majority of the biomass in this system (Gradinger 2009), were melted with the addition of filtered seawater to
151 avoid osmotic stress (Garrison and Buck 1986). Half of the collected material was concentrated on a 20-µm sieve to
152 reduce liquid volume for transport (Gradinger et al. 2009). The inoculum was stored at 1 °C with 20 µmol photons
153 m^{-2} s^{-1}, until transport to Fairbanks where it was incubated under the same conditions. In addition, ice algae
154 samples were cultured at the University of Alaska Fairbanks from environmental samples collected earlier in the
155 year from fast ice close to Utqiaġvik with the addition of f/2 growth medium, aeration and continuous low light of
156 ~20 µmol photons m^{-2} s^{-1}. Cultured algae were mixed with the ice core inoculum to increase biomass.

157 The inoculum was added to each of the tanks after ice had grown to an initial thickness of 10 cm. Crushed
158 freshwater ice was mixed with half of the inoculum to create an ice slurry in an attempt to support the
159 incorporation of the collected biological material into the growing ice sheets by providing buoyant support for
160 biota. The inoculum was injected through a 5 cm diameter hole drilled through the ice in the center of each tank
161 and spread across the ice bottom using an L-shaped PVC device. After 24 hours, water pumps, used to disrupt the
162 formation of thermal convection cells in the tank, were temporarily turned off. A small hole (1.5 cm diameter) was
163 drilled through the ice close to the edge of the tank and the remaining inoculum, with a lower salinity relative to
164 tank water, was gently released in direct contact with the ice-water interface thus creating a stratified layer. The
165 inoculum was thereby held in close contact with the growing ice in order to promote movement of organisms into
166 the ice before pumps were turned back on four hours later.

167

168 *Treatments and Oil Release*

169 Following the initial biological inoculation, we incubated the tanks for 11 days for additional ice growth, algal
170 growth, and algal acclimation prior to the start of the exposure experiment. Failure of one BC tank occurred before
171 the onset of sampling and no data was recovered.

172 The six tanks were divided into three different treatments with two replicates each: 1) Biological Control (BC; no
173 oil), 2) Oil Lens (OL; 2L oil pooled under ice per tank) and 3) Physically Dispersed Oil (PD; 0.5 L oil under ice per
174 tank, mechanically emulsified and allowed to pool under the ice). Alaska North Slope (ANS) crude oil, collected
175 from Pump Station 1 at the Trans-Alaska Pipeline entry point (provided by Alyeska Pipeline Services), was used for
176 these experiments. Oil was pre-chilled (-2 °C) and injected by positive displacement of water for the OL
177 treatments, or by injection of 500 ml oil through a small impeller for the PD treatments.

178

179 *Sampling of sea ice from the tanks*

180 Ice cores were collected with a 5 cm inner-diameter stainless-steel corer (manufactured by UAF Geophysical
181 Institute Machine Shop). A minimum of 5 cm buffer zone was left between any two holes or structure transiting
182 the ice in order to minimize effects of enhanced brine drainage. A template of equally distributed coring locations
183 was used to maximize space efficiency; the location of each collected sample was then determined by random
184 selection without repeat. Brackish ice-plugs were cut to the corresponding ice thickness and used to fill holes after
185 core removal. Each replicate tank was sampled twice: two days prior to oil release (pre-oil) and 10 days after oil
186 release (post-oil). Three replicate cores for biological analyses, and two for bulk salinity measurements, were
187 removed at both sampling events from each tank. Salinity cores were immediately sectioned into 2.5 cm long
188 segments and stored at -20 °C in a sealed glass container until processing Total ice core length (ice thickness) was
189 measured prior to sectioning. The top 10 cm of each core was discarded, as it had grown prior to inoculation of
190 biota.

191 Pre-oil biological cores, taken prior to the oil release, were sectioned into two 5 cm segments (Fig. 2). Section
192 names were conserved across sampling days with the topmost section referred to as upper and the layer below it

as supra-oil (Fig. 2). Ice cores from one of the PD tanks were too short to yield a complete upper section so only the bottom 5 cm were taken from this core and it was analyzed as a supra-oil segment. The experiment was terminated after 10 days of oil exposure (post-oil sampling), at which time the same sections were taken as during the pre-oil sampling plus an additional section of the ice that had grown after oil introduction which we termed the sub-oil section (Fig. 2).

Determination of salinity, brine properties, algal abundance, EPS and Chl a concentrations

Bulk salinity was measured in directly melted ice core sections using a YSI EcoSense EC300A salinometer. Brine salinity and brine volume fraction (BVF) were calculated using the Cox and Weeks (1983) equations, based on the measured ice temperatures and bulk salinities.

Biological samples were melted in the dark at 3 °C with the addition of filtered seawater and immediately processed after complete melt (Garrison and Buck 1986). Melted samples containing oil required pre-treatment by aspiration of the oil lens, gentle homogenization, and transfer to a separatory flask through a large glass funnel, where part of the oil remained on the funnel through adhesion. The sample was then allowed to sit for 60 seconds as small oil droplets collected at the surface before being transferred into a new pre-cleaned container at a rate of approximately 1 l min^{-1}, removing much of the visible oil by adhesion to the separatory flask wall. Pre-oil and all BC samples did not contain oil and were therefore not subjected to this process. At this stage, all samples were gently homogenized and divided into three sub-samples for algal enumeration by epifluorescence and standard light microscopy, as well as determination of EPS and Chl *a* concentrations.

Taxonomic identification of algae was conducted for a small subsample from each tank using an inverted Zeiss light microscope. For algal abundance estimation, melted samples were fixed in brown amber glass bottles with formaldehyde (1% final concentration). Counting by epifluorescence microscopy was carried out at 1,000x magnification using an Olympus BX51 microscope with UV light excitation (excitation: 330/80 nm, long pass: 400 nm) after DAPI (4', 6-diamidino-2-phenylindole) staining. Briefly, 10-50 ml of fixed sample was filtered onto a 0.2 µm Nuclepore filter atop a 0.8 µm supporting filter and stained with DAPI (0.1 µg ml^{-1} sample final concentration) for 5 minutes (Porter and Feig 1980). Cells were counted and categorized based on epifluorescence properties described in the results; empty diatom frustules were also enumerated.

For determination of EPS concentrations, melted ice samples were filtered directly onto 25 mm-diameter 0.4 µm polycarbonate membrane filters and EPS was extracted using the phenol-sulfuric acid method (DuBois et al. 1956). Absorbance measurements for EPS analysis were conducted using a Molecular Devices SPECTRA max 340PC 96 well microplate reader. A standard curve was generated using D (+) Glucose yielding EPS concentration as Glucose Equivalents (GEQV). For comparability with the alternative Alcian Blue method of EPS determination (Alldredge et al. 1993) the GEQV (µg l^{-1} ice) concentrations were converted into Xanthan Gum Equivalents (µg XGEQV l^{-1} ice) according to van der Merwe et al. (2009), using:

$$XGEQV = 0.975 \times \mathrm{GEQV} + 0.879.$$

Melted ice samples for Chl *a* analysis were filtered onto Whatman GF/F filters, extracted in 90% acetone, and analyzed according to Arar and Collins (1997) using a Turner TD-700 fluorometer.

Calculation of light intensities under oil

All mesocosms were illuminated from above. Initially, PAR was measured under the ice in one BC tank, and adjusted daily to maintain a constant light intensity in the seawater below the ice of I = 15 µmol photons m^{-2} s^{-1}. However, this sensor failed, and we used previous experience to adjust for increased attenuation by increasing ice thickness by increasing the surface light intensity.

The additional attenuation of PAR due to the presence of an oil layer was estimated based on the Lambert Beer equation, where Z is the thickness of the oil layer, I is the light intensity, and k is the oil attenuation coefficient:

$$I_Z = I_0 \, e^{-kZ}$$

Two extinction coefficients (k) of crude oil at two different wavelengths (Chl *a* absorption maxima) were used with k values of 21.8 mm^{-1} at λ = 450 nm and 2.66 mm^{-1} at λ = 650 nm (Sierra 1972). Assuming an even distribution under the ice, the applied 2 l oil lens treatment would have resulted in an average lens thickness of 5.6 mm, while the 0.5 l dispersed oil would have had a mean thickness of 1.4 mm. This simplified view does not account for variability of oil pooling under the ice. Variability in oil distribution was observed in sea-ice cores and larger ice-slabs removed at the end of the experiment. However, a more even distribution of oil was observed in the PD treatment. Redistribution of oil also occurred, seen as oil infiltration into the brine channel system, and percolation to the surface in the OL tanks. A more detailed description of oil movement in this experiment can be found in Oggier et al. (2019).

Statistical analyses

All statistical analyses were conducted using R version 3.6.1 (R Core Team 2019). Linear Mixed Effects Regression models (LMER, R package lme4 1.1-21; Bates et al. 2014) with and without treatment as a factor were compared using one-way ANOVA for each biological parameter, *i.e.* algal abundance, Chl *a*, and EPS across sections allowing for selection of the best model. All LMER models performed better including treatment. We chose LMER as it accounts for an unequal sample size, the repeated measures design, and the random effect that each tank has on biological concentrations and development. As a result, figures and means are represented by the least squared means generated by the LMER model (R package lsmeans 2.30-0; (Lenth 2016)). Pairwise comparison of least-squares means was used for post-hoc assignment.

Results

Temperature, bulk and brine salinity, and ice thickness

Thermistor strings embedded in the ice showed a linear temperature profile on each of the two sampling days (r^2>0.99) with lowest temperatures close to the ice surface, typical for growing ice sheets. Temperature in the ice remained stable throughout the duration of the experiment except during extensive sampling days when the ice warmed over a 24-hour period due to our activities (Online Resource 3). The brine salinity, estimated based on the ice temperature, was highest in the coldest ice sections, exceeding 100. The bulk salinities within the ice segments ranged from 4.0 to 12.5 with highest values in the bottom 5cm sections. The brine volume fraction showed similar maximum values prior to and following oil release with highest values (15 to 20% ice volume) in the bottom ice segments and decreasing values in the fresher and colder ice interior (Fig. 3). Ice thickness grew approximately 13 cm after initial sampling, and varied by tank (Table 1).

Algal abundance and species composition

The algal community in all treatments was dominated by the typical Arctic sea ice pennate diatom genus *Nitzschia* sp. (Fig. 4a, 99% total algal abundance), followed with very low abundances of the pennate diatom *Cylindrotheca closterium* (<1% contribution to total average abundance).

In all treatments, the highest abundance of diatom cells occurred in the lowermost 5 cm of the ice (Fig. 5a). Highest total diatom abundance exceeded 40 x 10^6 cells l^{-1} ice in the lowermost layer of the control treatment, while they never exceeded 14 x 10^6 cells l^{-1} ice in any of the oiled treatments. At the end of the experiment, the algal abundance in the lowermost ice section was significantly greater in the control (LMER, p<0.0001) compared to both oil treatments.

The diatom cells displayed two characteristically different fluorescence patterns (Fig. 4b & c; more examples found in Online Resource 4). Pattern 1 (P1) consisted of a combination of DAPI fluorescence of plastid DNA along the periphery of the plastid membrane, an elongated or irregularly shaped nucleus and an intact plasma membrane (Fig. 4b). Pattern 2 (P2) showed weak or no plastid DNA, a round nucleus and a disrupted plasma membrane (Fig.

4c). P1 cells dominated all treatments prior to oil release and in the control at the end of the experiment, averaged across all sections (Fig. 6). The relative abundance of P2 cells was similar for all replicates prior to oil release with an overall mean of 1.3 ± 1.5% of all cells and increased to the highest relative contribution of 54 ± 11% in the OL treatment, while it remained at 3.8 ± 3.9% in the control. The abundance of empty diatom frustules increased in all treatments over the course of the experiment from an initial average of 1.4 ± 0.1%, to a maximum value of 22 ± 7.5% in the PD treatment at the end of the experiment. The relative contribution of empty frustules was higher in the oiled treatments than the control (Fig. 6).

EPS concentrations

EPS concentrations prior to the oil release showed no vertical gradient in any treatment (Fig. 5b, white bars). Values ranged from 541 µg XGEQV l^{-1} ice to 743 µg XGEQV l^{-1} ice. The control treatment had a significantly higher EPS concentration in the sub-oil ice segment than in the oiled treatments (LMER, $p<0.05$; Fig. 5b).

Chlorophyll a concentrations

Pre-oil Chl *a* concentrations were not significantly different between upper and supra-oil sections in any treatment (Fig. 5c, white bars) with an overall mean value of 3.5 µg Chl *a* l^{-1} ice across all treatments. At the end of the experiment, the sub-oil ice Chl *a* concentration in the control was significantly higher compared to other sections and the sub-oil sections of the oiled treatments (LMER, $p<0.0001$; Fig. 5c) with values exceeding 75 µg Chl *a* l^{-1} ice.

Light attenuation by oil

Based on the attenuation modelling, the presence of oil strongly reduced (by 100-fold or more) the under-ice irradiance at wavelengths of maximum chlorophyll absorbance (Table 2). Assuming a similar reduction across the entire PAR spectrum would reduce the under-ice assumed light intensity to levels below the photosynthetic threshold except for the dispersed treatment at a wavelength of 650 nm. This calculation does not apply necessarily to all parts of the OL treatment tanks, as the oil had pooled in some areas, causing some removed ice cores to be free of oil.

We applied these attenuation factors to the natural environment, using incident irradiance across the PAR spectrum measured at Utqiaġvik, Alaska. We estimated the maximum oil layer thickness that would allow for photosynthesis to occur below the oil layer based on the lowest reported algal threshold irradiance of 0.17 (Hancke et al. 2018), and also 10 and 50 µmol photons m^{-2} s^{-1}: this lead to estimates of 3 mm thickness at the peak of the summer season, and around 1 and 2.5 mm during the spring and fall equinoxes, respectively (Fig. 7).

Discussion

Methodological constraints

Our experimental data demonstrate that it is experimentally possible to test for effects of oil exposure to sea ice biota under simulated *in situ* conditions in indoor ice tank mesocosms. They also provide clear evidence that crude oil exposure inhibited or reduced growth of ice algae in a sea-ice mesocosm as seen in three variables (algal abundance, Chl *a*, EPS).

While the experiments were conducted successfully, several methodological constraints must be considered. First, we did not replicate the natural diversity of ice algal communities in our tanks, which were dominated by the *Nitzschia sp.* However, this genus, and specifically the species *Nitzschia frigida*, is among the most common and abundant taxa found in Arctic sea ice (Hop et al. 2020), and is therefore a reasonable representation of natural sea ice communities. A similar diatom dominance at the end of an outdoor mesocosm study Weissenberger and Grossmann (1998) was observed, with a shift from initial dominance by flagellates, to the genus *Nitzschia*. We

suggest that future studies could avoid labor intensive field collections and increase the reproducibility of their research by seeding tanks with a single species of *Nitzschia* (e.g. *N. frigida*).

The use of LED lighting was a clear improvement compared to earlier studies, where the output of neon lighting had been temperature dependent in the cold rooms. This change in lighting system might also explain why we observed algal growth during periods of ice growth in our tanks, whereas a similar study Krembs et al. (2001) observed Chl *a* concentration increases only during a warming phase combined with higher light intensities.

The number of replicates in our study was limited due to the availability of cold room space, reducing the statistical power of our results, which was exacerbated by the failure of one control tank. Nevertheless, the magnitude of the difference between controls and oiled tanks in the biological properties was large enough to detect statistically significant differences. The small differences between the two oil treatments indicates, that a reduction in the number of treatments could be used to increase the number of treatments if the number of mesocosms is limiting. Experimental designs using outdoor tanks (as in Weissenberger 1998) or mesocosms (as in Camus and Smit 2019) allow for a considerable increase in replication or treatment by avoiding space limitations, but require a cold climate and are impacted by natural fluctuations of light and temperature. However, these designs would allow for a considerable increase in replication or treatment.

The detection of differences in cellular fluorescence between control and oiled treatments was an unexpected outcome of this study. Here we suggest that future studies include viability stains like SYTOX Green (Zetsche and Meysman 2012), which would allow for rapid assessment of cell status by flow cytometry (see discussion further below).

Algal pigment concentrations and cell counts, as measured in our study, are mandated by the National Oceanic and Atmospheric Administration's guidelines for Arctic oil spill assessment (Bejarano et al. 2014). Our study supports the continued use of these variables to assess oil spill impacts. Additionally, we propose that measures of cell viability could be usefully incorporated into oil spill assessments to detect sub-lethal effects on sea-ice algae that may be missed using only algal pigments and abundance.

Despite substantial differences in oiling regimes between the two different oiled treatments in this study, no significant differences in measurable biological effects were observed, leading to rejection of our second hypothesis. However, longer experiments may have elucidated differences in oil toxicity, or light availability, between these treatments, as observed during long term exposures to sub-lethal doses of WAF in *Boreogadus saida* (Bender et al. 2018). The presence of living cells in all core segments in this study suggest that algal survival was not completely inhibited by oil, so we recommend future experiments use varying concentrations of WAF to determine effect thresholds for important sea-ice autotrophs.

Longer experimental studies would also be needed to include the potential role of photooxidation and biodegradation for removal of oil spills as indicated in a 2.5 month long study in a first year ice area in Greenland, where removal rates were in the order of 1% per day (Vergeynst et al. 2019)

Reduction of algal growth and exudation

The reduced growth of ice algae, independent of the type of oil treatment, is a key finding of this experiment. Reduced growth was evidenced by three variables (cell abundance, Chl *a*, and EPS), but the underlying cause of this reduction could have multiple explanations. Here we evaluate the potential effects of light level, algal movement, and oil toxicity on the observed reductions in ice algal growth.

The presence of light-absorbing oil strongly reduced the under-ice irradiance available for photosynthesis to levels below those necessary to sustain algal growth in the oiled tanks based on the attenuation model. Uneven distribution of the oil either in smaller droplets or through variation in layer thickness (as observed for the OL treatment) could have caused heterogenous light levels in the tanks. Nevertheless, we suggest that shading due to entrained crude oil will reduce sea-ice algae productivity similar to the shading caused by the incorporation of sediments into sea ice (Gradinger et al. 2009). Based on light absorption models, a 2-33 mm thick oil layer may be sufficient to prevent photosynthesis in the ice in summertime Arctic conditions. In a real-world scenario, this translates to 1 m^3 of crude oil having the capacity to inhibit photosynthesis across 500 m^2 of sea ice. To put this in

perspective, community resupply tankers in the Arctic regularly carry over 5,000 m^3 of crude oil – enough to inhibit growth over an area of 2.5 km^2. However, as in our tanks, oil pooling under sea ice should accumulate in recessed undulations (Werner and Lindemann 1997), allowing for the potential of thick oil lenses directly adjacent to optically clear ice, causing increased ice algal patchiness and reduced total ice algal production in the area.

An additional non-lethal effect of an oil layer could be its impact on ice algal movement. Raphid pennate diatoms are able to adjust their position within the ice by gliding movement (Aumack et al. 2014), which could be inhibited by the presence of an oil layer. Such an oil barrier would limit the ability of taxa to follow the growing ice front, causing them to become entrapped in the ice interior with sub-optimal conditions for temperature, brine salinity and nutrient supply. Microorganisms including algae are already entrained during the early growth of sea ice (especially during frazil ice formation) and much less so during columnar ice formation (Gradinger and Ikävalko 1998; Collins et al. 2010) pointing towards the importance of organismal movement within the ice. We did observe intact algae in the bottom section formed after the oil release. We cannot however distinguish whether they reached the newly formed bottom layer through movement within the ice or whether new entrainment from the water column occurred as recently suggested for older stages of sea ice (Olsen et al. 2017).

Direct toxic effects of crude oil and its distillates on phytoplankton cell division and growth are well established (Hsiao 1978; Aksmann and Tukaj 2008; Gilde and Pinckney 2012) and may explain the reduced abundances, EPS and Chl *a* concentrations we observed in oiled treatments. Microbial communities, predominantly diatoms in sea ice, exudate EPS which accumulates to high concentrations (Krembs et al. 2002; Aslam et al. 2016). We observed highest EPS concentrations in the control treatment, suggesting a production by the also higher algal biomass in this treatment. Interestingly, bacteria and microalgae use EPS as protection against heavy metals (Bitton and Freihofer 1978; Serra et al. 2009; Sousa et al. 2019), but we did not find an increased production in our oiled treatments in response to oil exposure. The EPS concentrations in our tanks were similar to field conditions prior to a spring bloom, i.e., up to mid-March under low snow or mid-May under high snow cover (Riedel et al. 2006). It remains possible EPS can offer a protective barrier to crude-oil toxicity at higher concentration of EPS, or lower concentrations of oil, and that increased porosity caused by EPS could increase oil infiltration into the ice thus increasing exposure.

Toxicity effects in phytoplankton can vary dependent on species and community composition (Gilde and Pinckney 2012; Özhan et al. 2014). Of the major microalgae groups, diatoms dominated in our tanks and are sensitive to the effect of crude oils (Hsiao 1978; Perez et al. 2010; Podkuiko 2013; Finkel et al. 2020) rendering ice-algal communities particularly at risk given they are often dominated by diatoms (Szymanski and Gradinger 2016). These previous studies observed species shifts from diatoms to flagellates after oil spills in phytoplankton communities, which we did not observe in our study. The response of species to oil exposure is also not a constant but varies with their physiological state, e.g., nutrient limitation. Cell size and its surface to volume ratio also is relevant, initially suggesting increased sensitivity of smaller cells to oil exposure (Echeveste et al. 2010). However, field data and experiments also observed the opposite trend with stimulation of small diatoms (<20 µm) by oil exposure while negative effects occurred for large diatoms (>20 µm) (González et al. 2009). This discrepancy between studies expresses the importance of establishing species or community specific responses to oil exposure before developing threshold levels for assessment and mitigation frameworks. It can be expected that responses of the highly diverse communities occurring in natural sea ice (Poulin et al. 2011) will be more complex than those observed in our study, and therefore diversity measures should be included in such field based or large mesocosm studies.

Indicators of cell damage and mortality

Clear evidence for oil toxicity effects at the cellular level arose from the observed increase in the frequency of empty diatom frustules, and the change in cellular fluorescence. The relative frequency of empty diatom frustules had earlier been suggested for planktonic communities by Echeveste et al. (2010) and Gilde and Pinckney (2012). It may be a specifically suitable metric for sea-ice communities because they are often dominated by diatoms as main primary producers while planktonic communities under Arctic sea ice are often dominated by flagellated taxa without hard structures (Balzano et al. 2012). Field observations (Gradinger unpubl.) suggest that empty silicate

frustules are retained within the ice matrix after natural diatom cell death, another prerequisite to applying this approach in sea ice. While the relative empty frustule abundance can be caused by the toxicity of oiling, natural cell death can occur either due to severe environmental stress within the ice system or through, e.g., fungal infections (Hassett et al. 2019) or meiofaunal grazing.

We were initially surprised to observe the differences between the two DAPI fluorescence patterns P1 and P2. The fluorescent dye DAPI binds to nucleic acids (primarily DNA but also to RNA) and stains plastid (Selldén and Leech 1981), mitochondrial (Williamson and Fennell 1979) and nuclear DNA (Porter and Feig 1980). Current viability assays of phytoplankton rely on specific stains (Roth et al. 1997; Veldhuis et al. 2001; Echeveste et al. 2010) or digestive enzymes (Agusti and Sánchez 2002) that penetrate compromised cell membranes for easy viewing in unfixed samples. These assays do not work with fixed samples, because once the cells are preserved in formaldehyde, the plasma membrane becomes permeable within 20 to 120 minutes (Veldhuis et al. 2001), while the DAPI staining happens after fixation.

We established that oiled tanks had significantly higher proportions of diatom cells showing fluorescence pattern P2, i.e., lack of plastid DNA fluorescence and a round nucleus, while the control remained relatively unchanged. Diatom nuclei are predominately "pillow-like" or spherical in shape; the occurrence of many other irregular shapes can increase surface contact of cell organelles by means of nuclear pores (Bedoshvili and Likhoshway 2012). Our study presents evidence for oil-induced changes to nuclear shape in *Nitzschia* sp., and potentially this could be used as a routine measure to detect toxicity effects. Nuclear shape is used as a routine method to detect disease in humans (Webster et al. 2009). Veldhuis et al. (2001) determined phytoplankton cells retain their photopigments and that loss of membrane integrity occurs over several days under normal conditions as a process of unicellular automortality, synonymous to apoptosis in multicellular organisms. This suggests that there may be a delayed response of nucleus shape to oil exposure. While this DAPI staining post-fixation approach would simplify the detection of cellular effects, it requires validation across several microalgal groups.

In conclusion, our study clearly demonstrates the feasibility of ice tank studies for testing the effects of pollutants on ice communities. We believe that such studies are necessary to approach the role of pollutants in general in the highly structured sea ice system. The experiment demonstrates the complexity of ice algal oil-impact assessments and the need for cell mortality determination. Although challenging to set up and maintain, sea ice mesocosm experiments should continue to act as an important method for testing the effects of environmentally destructive drivers of algal productivity or other biotic metrics relevant to sea ice rather than testing isolated ice biota from their habitat. We recommend increased number of replicates, fewer treatments, and stronger focus on indicators of cell viability and sub-lethal effects to be included in future studies.

Author Contributions

The author team conceived the study idea and obtained the funding. KD and MO designed and constructed the experimental tanks, and conducted the field work and experiments. KD subsequently processed the biological samples that form the core of the article, and analyzed the resulting data, advised by RG and BB. KD, BB and RG prepared the first draft of the manuscript which all authors then improved, edited and approved. KD and RG revised the reviewed manuscript.

Acknowledgements

We thank Ukpeaġvik Iñupiat Corporation (UIC) Science for their logistical support in Utqiaġvik during field work. Matthew Balazs (University of Alaska Fairbanks, UAF), Michael Donovan and Michael Thomas (UIC) provided support in the field. We thank Mette Kauffman, Alexis Walker, and the many contributors who volunteered their time to assist with laboratory work. We would like to thank Pedro Echeveste and two anonymous reviewers for the constructive critique that improved this article. This project was funded by a research grant provided through the Coastal Marine Institute (CMI M14AC00015), a joint institute between the Bureau of Ocean Energy Management (BOEM) and the University of Alaska Fairbanks (UAF). Additional financial support was provided by the Robert and Kathleen Byrd Award. The basis for this publication is the first author's Master thesis. Data are available from the figshare data repository at (doi: 10.6084/m9.figshare.11918349).

References

Agusti S, Sánchez MC (2002) Cell variability in natural phytoplankton communities quantified by a membrane permeability probe. Limnol Oceanogr 47:818–828.

Aksmann A, Tukaj Z (2008) Intact anthracene inhibits photosynthesis in algal cells: A fluorescence induction study on *Chlamydomonas reinhardtii* cw92 strain. Chemosphere 74:26–32. https://doi.org/10.1016/j.chemosphere.2008.09.064

Alldredge AL, Passow U, Logan BE (1993) The abundance and significance of a class of large, transparent organic particles in the ocean. Deep-Sea Res Pt I 40:1131–1140. https://doi.org/10.1016/0967-0637(93)90129-Q

Arar EJ, Collins GB (1997) In vitro determination of chlorophyll *a* and phaeophytin *a* in marine and freshwater by fluorescence, Method 445.0. National Exposure Research Laboratory, US EPA, Cincinnati

Arctic Council (2009) Arctic Marine Shipping Assessment 2009 Report

Aslam SN, Cresswell-Maynard T, Thomas DN, Underwood GJC (2012) Production and characterization of the intra- and extracellular carbohydrates and polymeric substances (EPS) of three sea-ice diatom species, and evidence for a cryoprotective role for EPS. J Phycol 48:1494–1509. https://doi.org/10.1111/jpy.12004

Aslam SN, Michel C, Niemi A, Underwood GJC (2016) Patterns and drivers of carbohydrate budgets in ice algal assemblages from first year Arctic sea ice. Limnol Oceanogr 61:919–937. https://doi.org/10.1002/lno.10260

Aumack CF, Juhl AR, Krembs C (2014) Diatom vertical migration within land-fast Arctic sea ice. J Marine Syst 139:496–504. https://doi.org/10.1016/j.jmarsys.2014.08.013

Balzano S, Gourvil P, Siano R, Chanoine M, Marie D, Lessard S, Sarno D, Vaulot D (2012) Diversity of cultured photosynthetic flagellates in the northeast Pacific and Arctic Oceans in summer. Biogeosciences 9:4553–4571. https://doi.org/10.5194/bg-9-4553-2012

Bates D, Mächler M, Bolker B, Walker S (2015) Fitting linear mixed-effects models using lme4. J Stat Softw 67:1–51. https://doi.org/10.18637/jss.v067.i01

Bedoshvili Y, Likhoshway Y (2012) The cell ultrastructure of diatoms - implications for phylogeny? In: The Transmission Electron Microscope. Book, pp 147–160.

Bejarano AC, Michel J, Allan SE (2014) Guidelines for collecting high priority ephemeral data for oil spills in the Arctic in support of natural resource damage assessments. Report.

Bender ML, Frantzen M, Camus L, Le Floch S, Palerud J, Nahrgang J (2018) Effects of acute exposure to dispersed oil and burned oil residue on long-term survival, growth, and reproductive development in polar cod (*Boreogadus saida*). Mar Environ Res 140:468–477. https://doi.org/10.1016/j.marenvres.2018.09.005

Bitton G, Freihofer V (1978) Influence of extracellular polysaccharides on the toxicity of copper and cadmium toward *Klebsiella aerogenes*. Microb Ecol 4:119–125.

Bluhm BA, Hop H, Vihtakari M, Gradinger R, Iken K, Melnikov IA, Søreide JE (2018) Sea ice meiofauna distribution on local to pan-Arctic scales. Ecol Evol 2350–2364. https://doi.org/10.1002/ece3.3797

BOEM (2019) 2019-2024 Draft Proposed Program Lease Sale Schedule. https://www.boem.gov/sites/default/files/oil-and-gas-energy-program/Leasing/Five-Year-Program/2019-2024/DPP/NP-DPP-Lease-Sale-Schedule-2019-2024.pdf

Boetius A, Albrecht S, Bakker K, Bienhold C, Felden J, Fernandez-Mendez M, Hendricks S, Katlein C, Lalande C, Krumpen T, Nicolaus M, Peeken I, Rabe B, Rogacheva A, Rybakova E, Somavilla R, Wenzhofer F (2013) Export of algal biomass from the melting Arctic sea ice. Science 339:1430–1432. https://doi.org/10.1126/science.1231346

Buist IA, Dickins DF (1987) Experimental spills of crude oil in pack ice. Int Oil Spill Conf Proc 1987:373–381. https://doi.org/10.7901/2169-3358-1987-1-373

Camus L, Smit M (2019) Environmental effects of Arctic oil spills and spill response technologies, introduction to a 5 year joint industry effort. Mar Environ Res 144:250–254. https://doi.org/10.1016/j.marenvres.2017.12.008

Collins RE, Rocap G, Deming JW (2010) Persistence of bacterial and archaeal communities in sea ice through an Arctic winter. Environ Microbiol 12:1828–1841. https://doi.org/10.1111/j.1462-2920.2010.02179.x

Cox GFN, Weeks WF (1983) Equations for determining the gas and brine volumes in sea ice samples. J Glaciol 29:306–316. https://doi.org/10.3198/1983JoG29-102-306-316

Cross WE, Martin CM (1987) Effects of oil and chemically treated oil on nearshore under-ice meiofauna studied in situ. Arctic 40:258–265.

Dickens D, Overall J, Brown R (1975) The Interaction of Crude Oil with Arctic Sea Ice. Report.

DuBois M, Gilles K a., Hamilton JK, Rebers P a., Smith F (1956) Colorimetric method for determination of sugars and related substances. Anal Chem 28:350–356. https://doi.org/10.1021/ac60111a017

Echeveste P, Agustí S, Dachs J (2010) Cell size dependent toxicity thresholds of polycyclic aromatic hydrocarbons to natural and cultured phytoplankton populations. Environ Pollut 158:299–307. https://doi.org/10.1016/j.envpol.2009.07.006

Eguíluz VM, Fernández-Gracia J, Irigoien X, Duarte CM (2016) A quantitative assessment of Arctic shipping in 2010-2014. Sci Rep-UK 6:3–8. https://doi.org/10.1038/srep30682

Fiala M, Delille D (1999) Annual changes of microalgae biomass in Antarctic sea ice contaminated by crude oil and diesel fuel. Polar Biol 21:391–396. https://doi.org/10.1007/s003000050378

Finkel Z V., Liang Y, Nanjappa D, Bretherton L, Brown CM, Quigg A, Irwin AJ (2020) A ribosomal sequence-based oil sensitivity index for phytoplankton groups. Mar Pollut Bull 151:110798. https://doi.org/10.1016/j.marpolbul.2019.110798

Frederiksen M, Linnebjerg JF, Merkel FR, Wilhelm SI, Robertson GJ (2019) Quantifying the relative impact of hunting and oiling on Brünnich's guillemots in the North-west Atlantic. Polar Res 38: https://doi.org/10.33265/polar.v38.3378

Gardiner WW, Word JQ, Word JD, Perkins R a, McFarlin KM, Hester BW, Word LS, Ray CM (2013) The acute toxicity of chemically and physically dispersed crude oil to key Arctic species under Arctic conditions during the open water season. Environ Toxicol Chem 32:2284–300. https://doi.org/10.1002/etc.2307

Garrison DL, Buck KR (1986) Organism losses during ice melting: A serious bias in sea ice community studies. Polar Biol 6:237–239. https://doi.org/10.1007/BF00443401

Gilde K, Pinckney JL (2012) Sublethal effects of crude oil on the community structure of estuarine phytoplankton. Estuar Coast 35:853–861. https://doi.org/10.1007/s12237-011-9473-8

Glaeser JL, Vance GP (1971) A study of the behavior of oil spills in the Arctic. Report.

González J, Figueiras FG, Aranguren-Gassis M, Crespo BG, Fernández E, Morán XAG, Nieto-Cid M (2009) Effect of a simulated oil spill on natural assemblages of marine phytoplankton enclosed in microcosms. Estuar Coast Shelf Sci 83:265–276. https://doi.org/10.1016/j.ecss.2009.04.001

Gradinger R (2009) Sea-ice algae: Major contributors to primary production and algal biomass in the Chukchi and Beaufort Seas during May/June 2002. Deep-Sea Res Pt II 56:1201–1212. https://doi.org/10.1016/j.dsr2.2008.10.016

Gradinger R, Bluhm B (2020) First Arctic sea ice meiofauna food web analysis based on abundance, biomass and stable isotope ratios of sea ice metazoan fauna from near-shore Arctic fast ice. Mar Ecol Prog Ser 634:29–43. https://doi.org/10.3354/meps13170

Gradinger R, Ikävalko J (1998) Organism incorporation into newly forming Arctic sea ice in the Greenland Sea. J Plankton Res 20:871–886. https://doi.org/10.1093/plankt/20.5.871

Gradinger R, Kaufman M, Bluhm B (2009) Pivotal role of sea ice sediments in the seasonal development of near-shore Arctic fast ice biota. Mar Ecol Prog Ser 394:49–63. https://doi.org/10.3354/meps08320

Hancke K, Lund-Hansen LC, Lamare ML, Højlund Pedersen S, King MD, Andersen P, Sorrell BK (2018) Extreme low light requirement for algae growth underneath sea ice: a case study from Station Nord, NE Greenland. J Geophys Res-Oceans 123:985–1000. https://doi.org/10.1002/2017JC013263

Hassett BT, Borrego EJ, Vonnahme TR, Rämä T, Kolomiets M V., Gradinger R (2019) Arctic marine fungi: biomass, functional genes, and putative ecological roles. ISME J 13:1484–1496. https://doi.org/10.1038/s41396-019-0368-1

Helle I, Mäkinen J, Nevalainen M, Afenyo M, Vanhatalo J (2020) Impacts of oil spills on Arctic marine ecosystems: A quantitative and probabilistic risk assessment perspective. Environ Sci Technol 54:2112–2121. https://doi.org/10.1021/acs.est.9b07086

Hop H, Vihtakari M, Bluhm BA, Assmy P, Poulin M, Gradinger R, Peeken I, Quillfeldt C, Olsen L, Zhitina L, Melnikov I (2020) Changes in sea-ice protist diversity with declining sea ice in the arctic ocean from the 1980s to 2010s. Front Mar Sci 7:1–18. https://doi.org/10.3389/fmars.2020.00243

Hsiao SC (1978) Effects of crude oils on the growth of Arctic marine phytoplankton. Environ Pollut 93–107.

Karlsson J (2009) A laboratory study of fixation, release rates and small scale movement of oil in sea ice. University of Copenhagen, Denmark. MS Thesis.

Krembs C, Eicken H, Deming JW (2011) Exopolymer alteration of physical properties of sea ice and implications for ice habitability and biogeochemistry in a warmer Arctic. P Natl Acad Sci USA 108:3653–8. https://doi.org/10.1073/pnas.1100701108

Krembs C, Eicken H, Junge K, Deming JW (2002) High concentrations of exopolymeric substances in Arctic winter sea ice: Implications for the polar ocean carbon cycle and cryoprotection of diatoms. Deep-Sea Res Pt I 49:2163–2181. https://doi.org/10.1016/S0967-0637(02)00122-X

Krembs C, Mock T, Gradinger R (2001) A mesocosm study of physical-biological interactions in artificial sea ice: Effects of brine channel surface evolution and brine movement on algal biomass. Polar Biol 24:356–364. https://doi.org/10.1007/s003000000219

Lee K, Li Z, Robinson B, Kepkay PE, Blouin M, Doyon B (2011) Field Trials of *in situ* Oil Spill Countermeasures in Ice-Infested Waters. Int Oil Spill Conf Proc. https://doi.org/10.7901/2169-3358-2011-1-160

Lee SH, Whitledge TE, Kang SH (2008) Spring time production of bottom ice algae in the landfast sea ice zone at Barrow, Alaska. J Exp Mar Biol Ecol 367:204–212. https://doi.org/10.1016/j.jembe.2008.09.018

Lemcke S, Holding J, Møller EF, Thyrring J, Gustavson K, Juul-Pedersen T, Sejr MK (2019) Acute oil exposure reduces physiological process rates in Arctic phyto- and zooplankton. Ecotoxicology 28:26–36. https://doi.org/10.1007/s10646-018-1995-4

Lenth R V. (2016) Least-squares means: The R package lsmeans. J Stat Softw 69: https://doi.org/10.18637/jss.v069.i01

Leu E, Mundy CJ, Assmy P, Campbell K, Gabrielsen TM, Gosselin M, Juul-Pedersen T, Gradinger R (2015) Arctic spring awakening - Steering principles behind the phenology of vernal ice algal blooms. Prog Oceanogr 139:151–170. https://doi.org/10.1016/j.pocean.2015.07.012

Liu SB, Chen XL, He HL, Zhang XY, Xie B Bin, Yu Y, Chen B, Zhou BC, Zhang YZ (2013) Structure and ecological roles of a novel exopolysaccharide from the Arctic sea ice bacterium *Pseudoalteromonas* sp. strain SM20310. Appl Environ Microbiol 79:224–230. https://doi.org/10.1128/AEM.01801-12

Mahoney AR, Eicken H, Gaylord AG, Gens R (2014) Landfast sea ice extent in the Chukchi and Beaufort Seas: The annual cycle and decadal variability. Cold Reg Sci Technol 103:41–56. https://doi.org/10.1016/j.coldregions.2014.03.003

Manes SS, Gradinger R (2009) Small scale vertical gradients of Arctic ice algal photophysiological properties. Photosynth Res 53–66. https://doi.org/10.1007/s11120-009-9489-0

Michel C, Ingram RG, Harris LR (2006) Variability in oceanographic and ecological processes in the Canadian Arctic Archipelago. Prog Oceanogr 71:379–401. https://doi.org/10.1016/j.pocean.2006.09.006

NEON (2020) National Ecological Observatory Network

Oggier M, Eicken H, Wilkinson JP, Petrich C, O'Sadnick M (2019) Crude oil migration in sea-ice: Laboratory studies of constraints on oil mobilization and seasonal evolution. Cold Reg Sci Technol 102924. https://doi.org/10.1016/j.coldregions.2019.102924

Olsen GH, Klok C, Hendriks AJ, Geraudie P, Hoop L De, Laender F De, Farmen E, Grøsvik BE, Hansen BH, Hjorth M, Jansen CR, Nordtug T, Ravagnan E, Viaene K, Carroll J (2013) Toxicity data for modeling impacts of oil components in an Arctic ecosystem. Mar Environ Res 90:9–17. https://doi.org/10.1016/j.marenvres.2013.05.007

Olsen LM, Laney SR, Duarte P, Kauko HM, Fernández-Méndez M, Mundy CJ, Rösel A, Meyer A, Itkin P, Cohen L, Peeken I, Tatarek A, Różańska-Pluta M, Wiktor J, Taskjelle T, Pavlov AK, Hudson SR, Granskog MA, Hop H, Assmy P (2017) The seeding of ice algal blooms in Arctic pack ice: The multiyear ice seed repository hypothesis. J Geophys Res-Biogeo 122:1529–1548. https://doi.org/10.1002/2016JG003668

Overland JE, Wang M (2013) When will the summer Arctic be nearly sea ice free? Geophys Res Lett 40:2097–2101. https://doi.org/10.1002/grl.50316

Özhan K, Miles SM, Gao H, Bargu S (2014) Relative phytoplankton growth responses to physically and chemically dispersed South Louisiana sweet crude oil. Environ Monit Assess 186:3941–3956. https://doi.org/10.1007/s10661-014-3670-4

Ozturk S, Aslim B (2010) Modification of exopolysaccharide composition and production by three cyanobacterial isolates under salt stress. Environ Sci Pollut Res 17:595–602. https://doi.org/10.1007/s11356-009-0233-2

Perez P, Fernandez E, Beiras R (2010) Fuel toxicity on *Isochrysis galbana* and a coastal phytoplankton assemblage: Growth rate vs. variable fluorescence. Ecotox Environ Saf 73:254–261. https://doi.org/10.1016/j.ecoenv.2009.11.010

Podkuiko L (2013) The effects of two crude oil solutions to phytoplankton species. Masters Thesis

Polyakov I V, Pnyushkov A V, Alkire MB, Ashik IM, Baumann TM, Carmack EC, Goszczko I, Guthrie J, Ivanov V V, Kanzow T, Krishfield R, Kwok R, Sundfjord A, Morison J, Rember R, Yulin A (2017) Greater role for Atlantic inflows on sea-ice loss in the Eurasian Basin of the Arctic Ocean. Science 356:285 LP – 291. https://doi.org/10.1126/science.aai8204

Porter KG, Feig YS (1980) The use of DAPI for identifying aquatic microfloral. Limnol Oceanogr 25:943–948. https://doi.org/10.4319/lo.1980.25.5.0943

Poulin M, Daugbjerg N, Gradinger R, Ilyash L, Ratkova T, von Quillfeldt C (2011) The pan-Arctic biodiversity of marine pelagic and sea-ice unicellular eukaryotes: A first-attempt assessment. Mar Biodivers 41:13–28. https://doi.org/10.1007/s12526-010-0058-8

Riedel A, Michel C, Gosselin M (2006) Seasonal study of sea-ice exopolymeric substances on the Mackenzie shelf: Implications for transport of sea-ice bacteria and algae. Aquat Microb Ecol 45:195–206. https://doi.org/10.3354/ame045195

Roth BL, Poot M, Yue ST, Millard PJ, Roth BL, Poot M, Yue ST, Millard PJ (1997) Bacterial viability and antibiotic susceptibility testing with SYTOX green nucleic acid stain. Appl Environ Microbiol 63:2421–2431.

Rysgaard S, Kühl M, Glud R, Würgler Hansen J (2001) Biomass, production and horizontal patchiness of sea ice algae in a high-Arctic fjord (Young Sound, NE Greenland). Mar Ecol Prog Ser 223:15–26. https://doi.org/10.3354/meps223015

Selldén G, Leech RM (1981) Localization of DNA in mature and young wheat chloroplasts using the fluorescent probe 4'-6-Diamidino-2-phenylindole. Plant Physiol 68:731–734. https://doi.org/10.1104/pp.68.3.731

Serra A, Corcoll N, Guasch H (2009) Copper accumulation and toxicity in fluvial periphyton: The influence of exposure history. Chemosphere 74:633–641. https://doi.org/10.1016/j.chemosphere.2008.10.036

Sierra JGO (1972) On the complex index of refraction for liquids. Missouri University of Science and Technology. MS Thesis.

Søreide JE, Leu E, Berge J, Graeve M, Falk-Petersen S (2010) Timing of blooms, algal food quality and *Calanus glacialis* reproduction and growth in a changing Arctic. Glob Change Biol 16:3154–3163. https://doi.org/10.1111/j.1365-2486.2010.02175.x

Sousa ML, Chow F, Pompêo MLM (2019) Community-level changes in periphytic biofilm caused by copper contamination. J Appl Phycol 31:2401–2410. https://doi.org/10.1007/s10811-019-1734-0

Szymanski A, Gradinger R (2016) The diversity, abundance and fate of ice algae and phytoplankton in the Bering Sea. Polar Biol 39:309–325. https://doi.org/10.1007/s00300-015-1783-z

Tkalich P, Chan ES (2002) Vertical mixing of oil droplets by breaking waves. Mar Pollut Bull 44:1219–1229. https://doi.org/10.1016/S0025-326X(02)00178-9

Toxværd K, Dinh K V, Henriksen O, Hjorth M, Nielsen TG (2019) Delayed effects of pyrene exposure during overwintering on the Arctic copepod *Calanus hyperboreus*. Aquat Toxicol 217:105332. https://doi.org/10.1016/j.aquatox.2019.105332

Underwood GJC, Aslam SN, Michel C, Niemi A, Norman L, Meiners KM, Laybourn-Parry J, Paterson H, Thomas DN (2013) Broad-scale predictability of carbohydrates and exopolymers in Antarctic and Arctic sea ice. P Natl Acad Sci USA 110:15734–9. https://doi.org/10.1073/pnas.1302870110

van der Merwe P, Lannuzel D, Nichols C a M, Meiners K, Heil P, Norman L, Thomas DN, Bowie a. R (2009) Biogeochemical observations during the winter-spring transition in East Antarctic sea ice: Evidence of iron and exopolysaccharide controls. Mar Chem 115:163–175. https://doi.org/10.1016/j.marchem.2009.08.001

Veldhuis M, Kraay G, Timmermans K (2001) Cell death in phytoplankton: correlation between changes in membrane permeability, photosynthetic activity, pigmentation and growth. Eur J Phycol 36:167–177. https://doi.org/10.1080/09670260110001735318

Vergeynst L, Christensen JH, Kjeldsen KU, Meire L, Boone W, Malmquist LMV, Rysgaard S (2019) In situ biodegradation, photooxidation and dissolution of petroleum compounds in Arctic seawater and sea ice. Water Res 148:459–468. https://doi.org/10.1016/j.watres.2018.10.066

Wang M, Yang Q, Overland JE, Stabeno P (2018) Sea-ice cover timing in the Pacific Arctic: The present and projections to mid-century by selected CMIP5 models. Deep-Sea Res Pt II 152:22–34. https://doi.org/10.1016/j.dsr2.2017.11.017

Webster M, Witkin KL, Cohen-Fix O (2009) Sizing up the nucleus: nuclear shape, size and nuclear-envelope assembly. J Cell Sci 122:1477–1486. https://doi.org/10.1242/jcs.037333

Weissenberger J (1998) Arctic Sea ice biota: Design and evaluation of a mesocosm experiment. Polar Biol 19:151–159. https://doi.org/10.1007/s003000050228

Weissenberger J, Grossmann S (1998) Experimental formation of sea ice: Importance of water circulation and wave action for incorporation of phytoplankton and bacteria. Polar Biol 20:178–188. https://doi.org/10.1007/s003000050294

Werner I, Lindemann F (1997) Video observations of the underside of Arctic sea ice-features and morphology on medium and small scales. Polar Res 16:27–36. https://doi.org/10.3402/polar.v16i1.6623

Wiedmann I, Ershova E, Bluhm BA, Nöthig EM, Gradinger RR, Kosobokova K, Boetius A (2020) What Feeds the Benthos in the Arctic Basins? Assembling a Carbon Budget for the Deep Arctic Ocean. Front Mar Sci 7:

https://doi.org/10.3389/fmars.2020.00224

Williamson DH, Fennell DJ (1979) Visualization of yeast mitochondrial DNA with the fluorescent stain "DAPI." Methods Enzymol 56:728–733. https://doi.org/10.1016/0076-6879(79)56065-0

Wilson RR, Perham C, French-mccay DP, Balouskus R (2018) Potential impacts of offshore oil spills on polar bears in the Chukchi Sea. Environ Pollut 235:652–659. https://doi.org/10.1016/j.envpol.2017.12.057

Zetsche EM, Meysman FJR (2012) Dead or alive? Viability assessment of micro- and mesoplankton. J Plankton Res 34:493–509. https://doi.org/10.1093/plankt/fbs018

Tables

Table 1 Average ice thickness and standard deviation at initial and final coring based on extracted core length for each of the three treatments, i.e., Physically Dispersed Oil (PD), Oil Lens (OL) and Biological Control (BC).

Treatment	Tank Replicate	Pre-Oil (cm)	Post-Oil (cm)
PD	1	19.3 ± 0.3	31.1 ± 0.5
PD	2	16.0 ± 1.7	26.6 ± 3.7
OL	1	20.0 ± 1.3	31.3 ± 1.1
OL	2	25.2 ± 2.7	40.2 ± 1.1
BC	1	18.4 ± 3.6	33.6 ± 1.1
All		**20.2 ± 3.6**	**33.0 ± 4.6**

Table 2 Calculated irradiance (µmol photons m^{-2} s^{-1}) under the oil layer in experimental tanks at wavelengths of 450 and 650 nm, the primary wavelengths of chlorophyll *a* absorbance, using calculated oil layer thicknesses. Treatments include Oil Lens (OL) and Physically Dispersed oil (PD) assuming an irradiance directly above the oil layer of 15 µmol photons m^{-2} s^{-1}.

Treatment	Estimated Oil Lens Thickness (mm)	Irradiance at 450 nm	Irradiance at 650 nm
OL	5.6	<0.001	<0.001
PD	1.4	<0.001	0.36

Figures

Fig. 1 Schematic of tank showing positions of sensors and equipment, as modified from Oggier et al. (2019). Letters represent: (a) LED light fixture, (b) datalogger, (c) thermistor chain, (d) temperature and salinity probe, (e) 4π PAR sensor, (f) circulation pump, (g) heater, (h) pressure release bladder; grey insulation represents 2 inch thick R10 foam surrounding the entire tank successfully hindering ice formation on the tank walls.

Fig. 2 Photographs of sea-ice cores extracted from tanks and their approximate core length (cm), with 0 indicating the ice-air interface. Sampling days were two days prior (Pre-Oil) and 10 days after (Post-Oil) oil release. Section names were conserved across sampling days and treatments, i.e., Physically Dispersed Oil (PD), Oil Lens (OL) and Biological Control (BC). The sub-oil is the layer of ice that continued to grow after the introduction of the oil; hence the oil layer is encapsulated into the ice. Sections denoted with an * were not sampled; dashed line represents the ice thickness at time of inoculation with biota. Solid lines indicate where cores were cut and the red indicates the oil release layer.

Fig. 3 Vertical profiles of measured bulk salinity, calculated brine salinity, and brine volume fraction (Cox and Weeks 1983) from ice cores collected pre- and post-oil release in each tank from the Physically Dispersed Oil (PD), Oil Lens (OL) and Biological Control (BC) treatments.

Fig. 4 Light transmittance micrograph of *Nitzschia* sp. from a Biological Control (BC) tank (panel a). Epifluorescent image of DAPI stained Pattern 1 (P1) diatom cells from BC treatment with plastid DNA (p) fluorescence along the periphery of the plastid membrane and an elongated or irregularly shaped nucleus (n; panel b). Epifluorescent image of DAPI stained Pattern 2 (P2) diatom cell from an oiled tank post-oil with tightly bundled, round, nucleus and disrupted plastid DNA fluorescence (panel c).

730 **Fig. 5** Mean values of diatom cell abundance (a), extracellular polymeric substances (EPS; b), and chlorophyll a (c)
731 of pseudo-replicate cores within treatments with 95% confidence intervals of each measured variable in Physically
732 Dispersed Oil (PD), Oil Lens (OL) and Biological Control (BC) treatments. Panels (top to bottom) represent vertical
733 stratigraphy of ice-core sections. Letters beside bars represent Tukey's post hoc group assignment.

734 **Fig. 6** Mean relative abundance of epifluorescent cell bins for all treatments, pre- and post-oil. Pattern 1 (P1),
735 Pattern 2 (P2), and frustules, are described in the methods and pictured in figure 2.

736 **Fig. 7** Estimated oil lens thicknesses that allow for under-oil irradiance of Photosynthetically Active Radiation (PAR;
737 400-700 nm) at 0.17, 10 and 50 µmol photons m^{-2} s^{-1} based on daily average PAR irradiance as recorded by the
738 Barrow Environmental Observatory (NEON 2020). 0.17 µmol photons m^{-2} s^{-1} is the minimum measured irradiance
739 for photosynthesis in Arctic sea-ice algae (Hancke et al. 2018). Calculated oil thickness only considers absorption at
740 650 nm which has the lowest extinction coefficient from 450-650 nm, therefore representing an idealized
741 situation (Sierra 1972).

742 **Electronic Supplemental Material 1** Ambient air and ice-surface temperature over the duration of the experiment.
743 Day is set relative to oil release (Day 0).

744 **Electronic Supplemental Material 2** Salinity measured from internally mounted salinometer sensor over the
745 duration of the experiment. Disruption of measurements occurred due to ice crystal formation on the sensors. Day
746 is set relative to oil release (Day 0).

747 **Electronic Supplemental Material 3** Hourly-averaged temperature field in tank for a replicate of the Oil Lens (OL)
748 treatment, from the ice surface (0 cm) to the bottommost temperature sensor (z = 32.5 cm). Day is set relative to
749 oil release (Day 0). The ice growth curve (dotted line) is the 2nd order best fit of the measured ice core length (•).
750 White-hatched area shows unavailable temperature data.

751 **Electronic Supplementary Material 4** Example binning from 10 epifluorescent micrographs. Red ellipses indicate a
752 cell representing the P2 classification -- tightly bundled, nucleus and disrupted plastid DNA fluorescence.

753

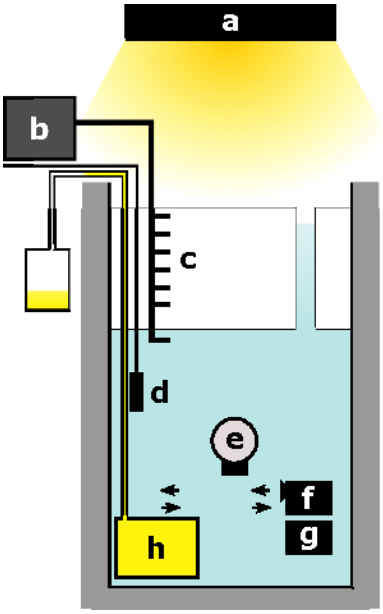

Figure 1

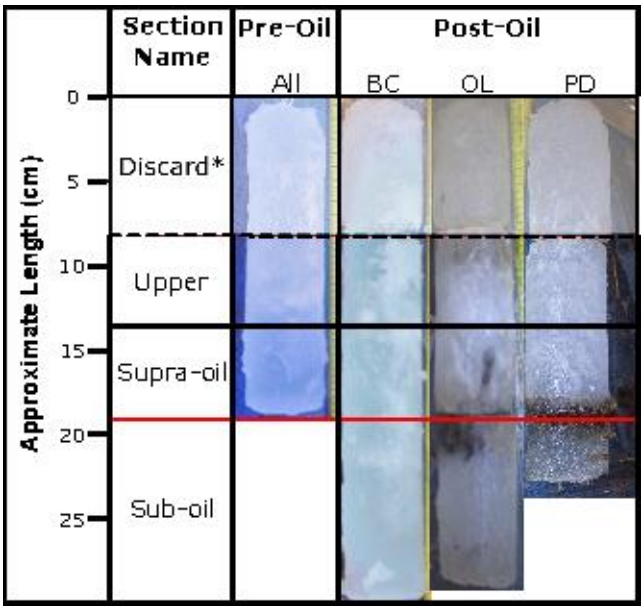

Figure 2

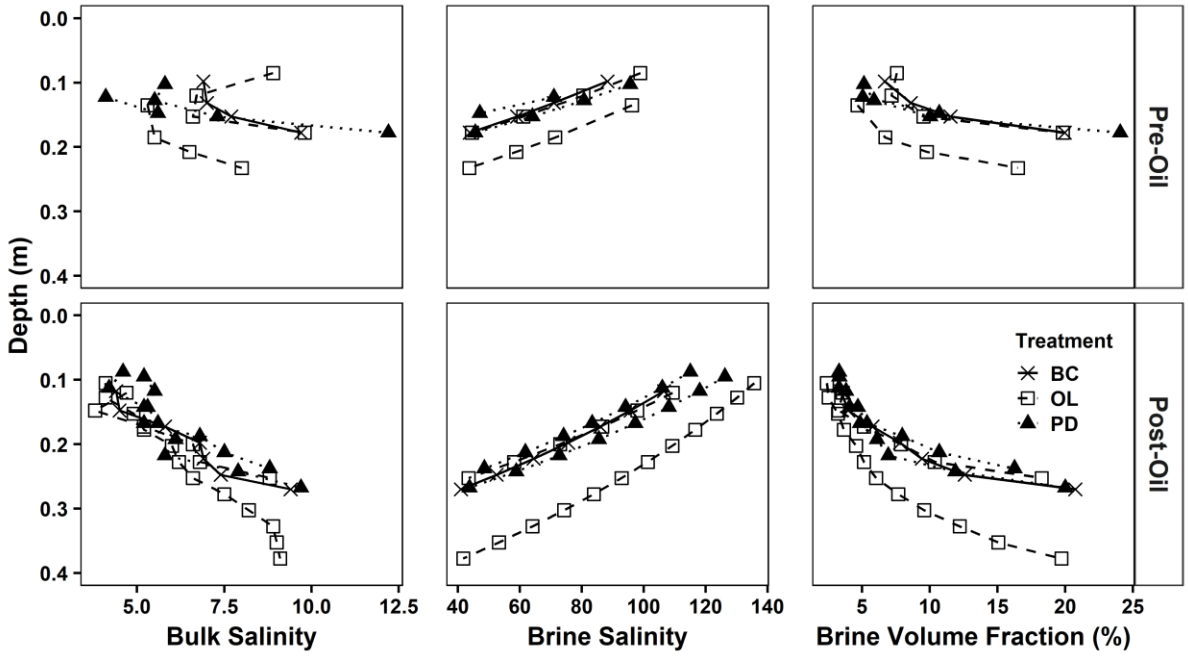

761

762 Figure 3

763

764

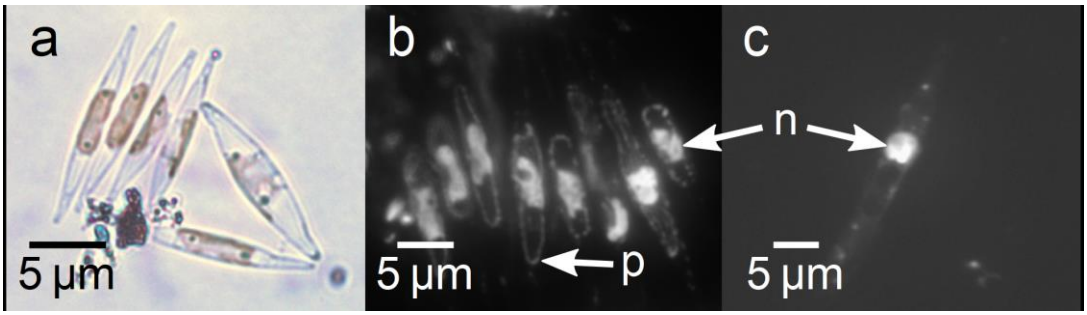

765

766 Figure 4

767

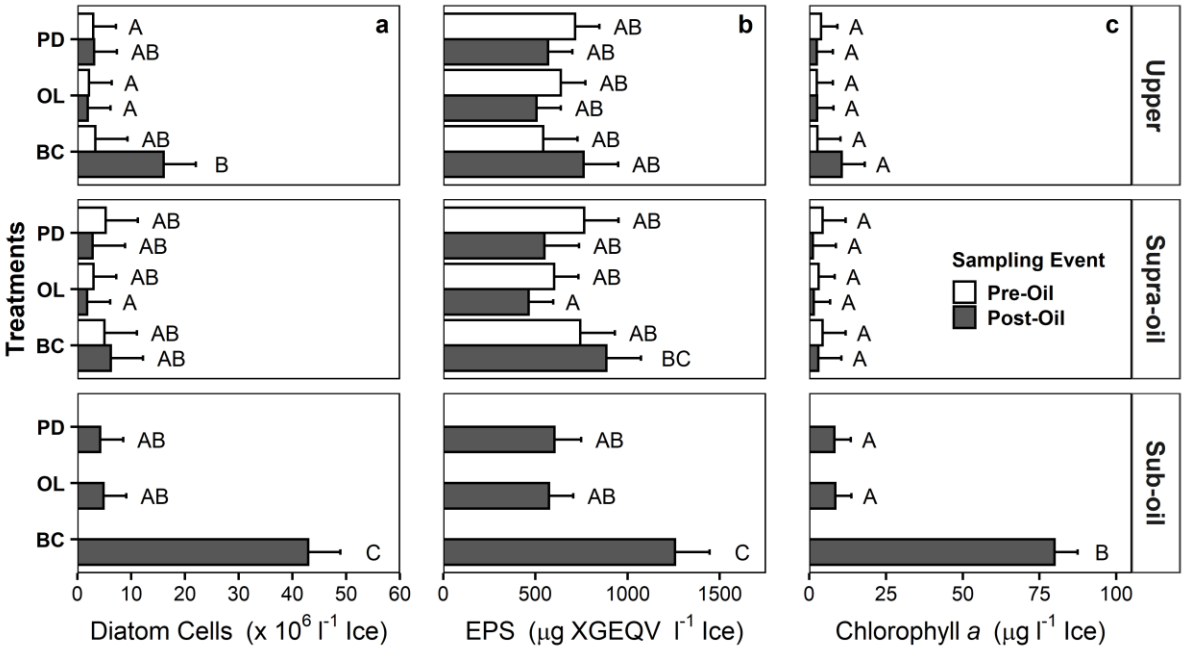

768

769 Figure 5

770

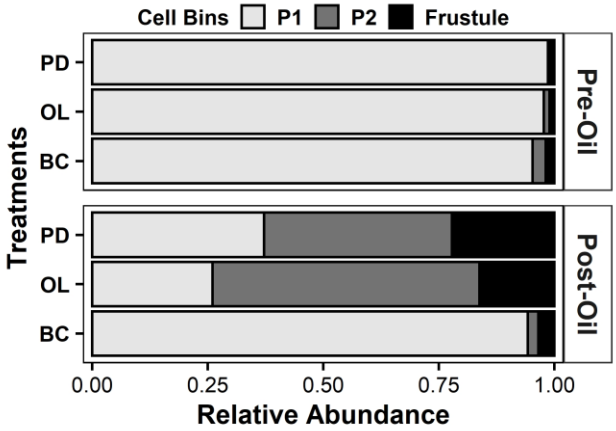

771

772 Figure 6

773

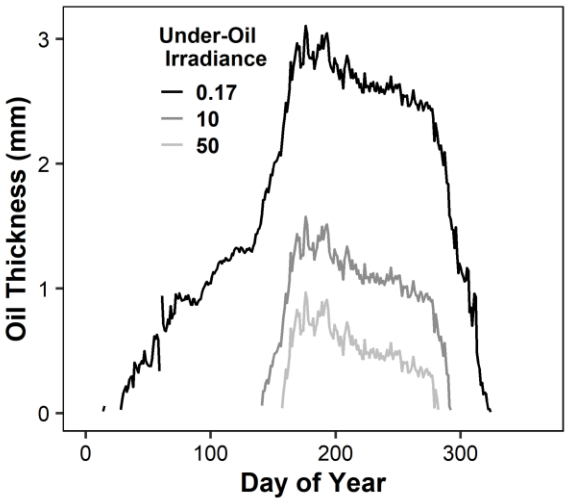

774

775 Figure 7